Communication

Conducting AFM and 2D GIXD Studies on Pentacene Thin Films

Hoichang Yang, Tae Joo Shin, Mang-Mang Ling, Kilwon Cho, Chang Y. Ryu, and Zhenan Bao

J. Am. Chem. Soc., **2005**, 127 (33), 11542-11543• DOI: 10.1021/ja052478e • Publication Date (Web): 30 July 2005

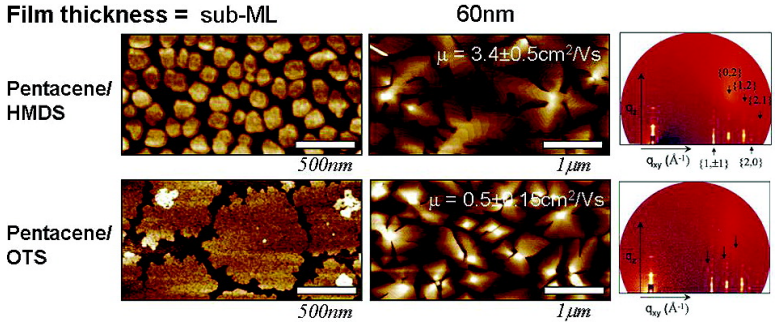

More About This Article

Additional resources and features associated with this article are available within the HTML version:

- Supporting Information
- Links to the 35 articles that cite this article, as of the time of this article download
- Access to high resolution figures
- Links to articles and content related to this article
- Copyright permission to reproduce figures and/or text from this article

View the Full Text HTML

J|A|C|S
COMMUNICATIONS

Published on Web 07/30/2005

Conducting AFM and 2D GIXD Studies on Pentacene Thin Films

Hoichang Yang,[†,||] Tae Joo Shin,[‡] Mang-Mang Ling,[§] Kilwon Cho,[||] Chang Y. Ryu,[†] and Zhenan Bao*[,§]

Rensselaer Nanotechnology Center, Rensselaer Polytechnic Institute, Troy, New York 12180, NSLS, Brookhaven National Laboratory, Upton, New York 11973, Department of Chemical Engineering, Stanford University, Stanford, California 94305, and Department of Chemical Engineering, Pohang University of Science and Technology, Pohang 790-784, Korea

Received April 16, 2005; E-mail: zbao@chemeng.stanford.edu

Among all organic semiconductors, pentacene has been shown to have the highest thin film mobility reported to date.[1−4] It is well-known that the charge carrier mobility of pentacene is sensitive to the surface properties of the dielectric layer. For example, Kelley et al. obtained high field effect mobility (~3 cm^2/Vs) with terrace-like pentacene multilayers on a 1-phosphoneo-hexadecane treated alumina dielectric layer.[1b] The molecular orientation and grain morphology of the first pentacene monolayer depend on pentacene−substrate interactions, which can be controlled by modification of the dielectric surface in an organic thin film transistor (OTFT) with a self-assembled monolayer (SAM).[2,3] Since the majority of charge carriers in an OTFT are located at the semiconductor−dielectric interface, this work focuses on the correlation between pentacene ultrathin film morphology and the overall OTFT device performance.[4] We found that there is a direct correlation between the crystalline structure of the initial submonolayer of a pentacene film and the mobility of the corresponding thick film. The terrace-like multilayered pentacene films, grown on single crystal-like faceted islands in the first layer, have shown much higher field-effect mobility than those grown on polycrystalline dendritic islands.

Ultrathin pentacene films (less than two monolayers (ML) < 3.2 nm) have recently been studied using atomic force microscopy (AFM) and grazing-incidence X-ray diffraction (GIXD).[2c] However, more detailed structural analyses using 2D GIXD in conjunction with conductivity studies using conducting AFM (C-AFM) of pentacene films have not been reported. Our work here is aimed at understanding how the crystalline morphology of the first layer ultimately influences the mobility of 60-nm pentacene films for OTFT applications. These films were prepared by vacuum-depositing pentacene at a rate of 0.5 Å/s on highly n-doped Si (with a thin layer of native oxide) or thermally grown SiO_2 on Si substrates, which had been pretreated with different types of SAMs: hexamethylene disilazane (HMDS) and octadecyltrimethoxy silane (OTS). The mobility of top contact OTFTs was measured using 60-nm-thick pentacene films.[4a] 2D GIXD and tapping mode AFM (TM-AFM) were employed to observe the crystalline morphology of multilayered pentacene films with different thicknesses, ranging from 2 ML to 60 nm (Supporting Information). Finally, C-AFM was used to study current flow through ultrathin pentacene layer(s) with different morphologies.

Figure 1 shows the 2D GIXD patterns and TM-AFM topographies for 60-nm-thick pentacene films deposited on HMDS- and OTS-treated surfaces. Many reflection spots in the direction of q_z (out-of-plane) at a given q_{xy} (in-plane) strongly suggest terrace-like 3D crystal formation of pentacene films in the vertical direction

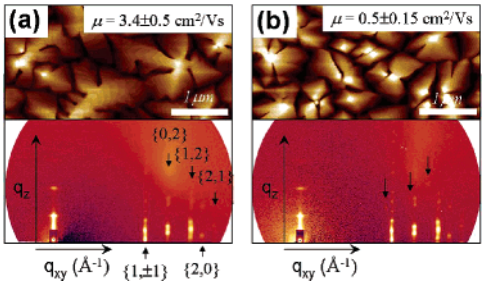

Figure 1. TM-AFM topographies and 2D GIXD patterns of 60-nm-thick pentacene films on (a) HMDS- and (b) OTS-treated SiO_2/Si substrates.

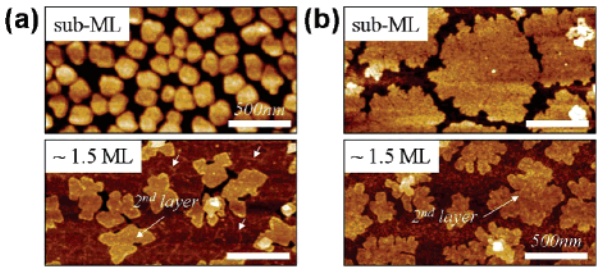

Figure 2. TM-AFM topographies for submonolayer and ~1.5 ML films on (a) HMDS- and (b) OTS-treated SiO_2/Si substrates.

as well as the lateral direction. Specifically, diffraction patterns of 2 ML pentacene films were indexed to a pseudo-centered rectangular unit cell ($a = 5.90 \pm 0.01$ Å, $b = 7.51 \pm 0.01$ Å, and $\gamma = 89.92 \pm 0.01°$) with a herringbone packing[2c] and molecules tilted along the *b*-axis by 4° with respect to the surface normal (Figure S1 in Supporting Information). Despite minute differences such as a small portion of different crystal orientation (indicated by black arrows in Figure 1b) and smaller grain size in the OTS sample, 2D GIXD supports the fact that the HMDS and OTS samples have a similar vertical conducting path for top contact devices. Mobility measurements, however, show drastically different mobilities: $\mu = 3.4 \pm 0.5$ cm^2/Vs on HMDS- and 0.5 ± 0.15 cm^2/Vs on OTS-treated surface, using 60-nm-thick pentacene films in the top contact OTFT.

Though TM-AFM topographies of pentacene films on hydrophilic O_2 plasma treated surfaces were not shown (Figure S2), we found that the overall surface coverage of the first layer was significantly improved by the hydrophobic SAM treatments[2] (Figure 2). A different level of surface roughness (Figure S3) from hydrophobic SAM treatment using HMDS or OTS was used to induce different nucleation and growth behavior in the first pentacene layer with similar surface coverage.[2c] As shown in Figure 2, faceted island morphology was observed for the pentacene sub-ML on a HMDS surface (roughness ≈ 0.5 nm), while dendritic

[†] Rensselaer Polytechnic Institute.
[‡] Brookhaven National Laboratory.
[§] Stanford University.
[||] Pohang University of Science and Technology.

10.1021/ja052478e CCC: $30.25

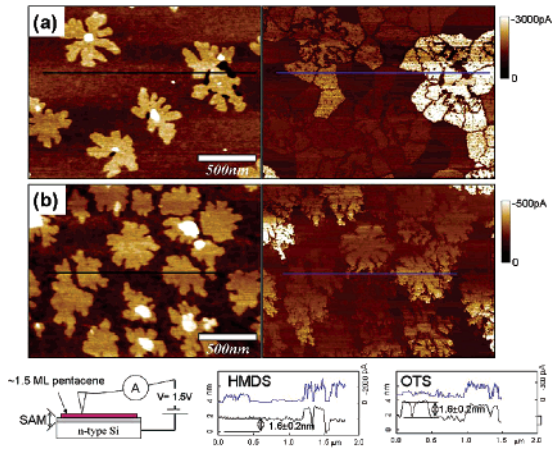

Figure 3. Simultaneously recorded contact topography (left) and C-AFM current (right) images for ~1.5 ML films on (a) HMDS- and (b) OTS-treated Si substrates. (The insets represent C-AFM experimental scheme, the cross-sectional profiles in topology, and C-AFM images, respectively.)

island morphology was found on the "smooth" OTS surface (roughness ≈ 0.1 nm). The faceted island on HMDS is reminiscent of the single crystal-like morphology of pentacene.[3a] On the contrary, the dendritic morphology represents a divergent polycrystalline growth initiated from a common nucleation point.[3b] The faceted or dendritic island morphology within the pentacene sub-ML has been maintained within the deposition rates from 0.1 to 0.5 Å/s (Figure S4). The TM-AFM images for ~1.5 ML pentacene films, however, show similar dendritic islands as the second layer grains on both HMDS- and OTS-treated surfaces. In addition, it was found that such morphological similarity persists for pentacene films thicker than 2 ML (Figure S5).

In recent studies about submonolayer growth of pentacene films based on simulation[2] and experiments,[2,3] it has been suggested that a slight change in deposition conditions has complex effects on the first layer morphology. Using 2D GIXD, we found that the uniform perpendicular pentacene orientation existed on both HMDS- and OTS-treated surfaces (Figure S6). Despite the similarity in molecular orientation, the morphological difference of the first layer islands greatly influences the structure of grain boundary (GB) within the first layer. In particular, the faceted-island morphology on HMDS had straight GBs, which were even discernible from TM-AFM images of ~1.5 ML film (white arrows in Figure 2). Because of the single crystal-like nature of the faceted islands, there would hardly be any internal defects during crystal packing in each grain. However, because of the morphological complexity of the dendrites, (i) two growing dendritic islands formed nonstraight GBs upon inter-island impingement and (ii) two adjacent dendrite branches also created intra-GBs within the island domains (Figure S7). Although the divergently growing pentacene dendrites formed larger individual islands resulting in fewer inter-GBs, they contained far more inter- and intra-GBs than the faceted islands. Therefore, the "overall" density of GBs within the first layer of pentacene should be much higher on OTS than on HMDS.

The C-AFM images strongly suggest that the morphology of the first and second pentacene monolayers plays a critical role in controlling the current flow through the pentacene layers between the AFM tip and the substrate. Using Pt/Cr-coated tips (diameter = 30 nm) under a +1.5 V bias on the substrate, we found that the faceted island grains on HMDS exhibited a 1 order of magnitude greater current than the dendritic grains on OTS. (Figure 3) This result is in good agreement with the charge mobility trend in OTFT devices with SAM layers. In addition, because the faceted islands formed straight GBs with less internal crystal defects, their GBs were clearly identified in C-AFM. The dendritic GBs, however, cannot be as clearly identified in C-AFM, presumably because of the high density of complex inter- and intra-GBs from branched dendritic islands.

The C-AFM current images showed that the second pentacene layer also played an important role in lateral charge transport across the first layer GBs by connecting the first faceted crystals. When the faceted island grains were connected above by the second layer, all connected grains in the first layer showed the same level of current flow. In contrast, when the first layer grains were distributed without connecting second layer islands, a mosaic-like current image exhibited that different levels of current flow were isolated and confined by the GB without the overbridging second layers.

In conclusion, 2D GIXD, TM-, and C-AFM analyses of pentacene films support the idea that the morphology of ultrathin layers plays a crucial role in determining mobility in OTFT. While 60-nm-thick pentacene films exhibited similar terrace-like multilayer structure with the long axis of pentacene perpendicularly oriented as determined from TM-AFM and 2D GIXD, its charge mobility in an OTFT was quite different, depending on the types of hydrophobic SAM surface treatment. This difference is related to the morphological difference of the first pentacene layer "buried" under the terrace-like multilayers. We found that the faceted islands on HMDS showed larger current flow than the dendritic islands on OTS using C-AFM. This trend in C-AFM current images correlated well with the charge carrier mobility measured in OTFTs. Such faceted morphology represents single crystal-like pentacene islands, which have fewer internal crystal defects and higher current flow than the dendritic islands.

Acknowledgment. H.Y. and K.C. thank the Ministry of Science and Technology of Korea (National Research Laboratory Program) for funding. Z.B. acknowledges partial financial support from 3M Faculty Award and Finmeccanica Faculty Scholar Award.

Supporting Information Available: Experimental methods, AFM images, 2D GIXD patterns, and X-ray analysis. This material is available free of charge via the Internet at http://pubs.acs.org.

References

(1) (a) Shtein, M.; Mapel, J.; Benziger, J. B.; Forrest, S. R. *Appl. Phys. Lett.* **2002**, *81*, 268. (b) Kelly, T.; Boardman, L. D.; Dunbar, T. D.; Muyres, D. V.; Pellerite, M. J.; Smith, T. P. *J. Phys. Chem. B* **2003**, *107*, 5877. (c) Dimitrakopoulos, C. D.; Malenfant, P. R. L. *Adv. Mater.* **2002**, *14*, 99. (d) Loi, M. A.; Como, E. D.; Dinelli, F.; Murgia, M.; Zamboni, R.; Biscarini, F.; Muccini, M. *Nat. Mater.* **2005**, *4*, 81. (e) Katz, H. E.; Bao, Z. *J. Phys. Chem. B* **2000**, *104*, 671. (f) Horowitz, G.; Hajlaoui, M. E. *Adv. Mater.* **2000**, *12*, 1046.

(2) (a) Ruiz, R.; Choudhary, D.; Nickel, B.; Toccoli, T.; Chang, K.; Mayer, A. C.; Clancy, P.; Blakely, J. M.; Headrick, R. L.; Iannotta, S.; Malliaras, G. G. *Chem. Mater.* **2004**, *16*, 4497. (b) Laquindanum, J. G.; Katz, H. E.; Dodabalapur, A.; Lovinger, A. *J. Am. Chem. Soc.* **1996**, *118*, 11331. (c) Fritz, S. E.; Martin, S. M.; Frisbie, C. D.; Ward, M. D.; Toney, M. F. *J. Am. Chem. Soc.* **2004**, *126*, 4084. (d) Fritz, S. E.; Kelley, T. W.; Frisbie, C. D. *J. Phys. Chem. B* **2005**, *109*, 10574. (e) Nickel, B.; Barabash, R.; Ruiz, R.; Koch, N.; Kahn, A.; Feldman, L. C.; Haglund, R. F.; Scoles, G. *Phys. Rev. B* **2004**, *70*, 125401.

(3) (a) Verlaak, S.; Steudel, S.; Heremans, P.; Janssen, D.; Deleuze, M. *Phys. Rev. B* **2003**, *68*. (b) Heringdorf, F. J. M. Z.; Reuter, M. C.; Tromp, R. M. *Nature* **2001**, *412*, 517. (c) Kasaya, M.; Tabata, H.; Kawai, T. *Surf. Sci.* **1998**, *400*, 367. (d) Pratontep, S.; Brinkmann, M.; Nuesch, F.; Zuppiroli, L. *Synth. Met.* **2004**, *146*, 387. (e) Lim, S. C.; Kim, S. H.; Lee, J. H.; Kim, M. K.; Kim, D. J.; Zyung, T. *Synth. Met.* **2005**, *148*, 75.

(4) (a) Ling, M. M.; Bao, Z. *Chem. Mater.* **2004**, *16*, 4824. (b) Jentzsch, T.; Juepner, H. J.; Brzezinka, K.-W.; Lau, A. *Thin Solid Films* **1998**, *315*, 273. (c) Knipp, D.; Street, R. A.; Volkel, A. R. *Appl. Phys. Lett.* **2003**, *82*, 390.

JA052478E